SHORT NOTES

Cladosporium species, a new challenge in strawberry production in Iran

Najmeh AYOUBI[1], Mohammad J. SOLEIMANI[1] and Rasoul ZARE[2]

[1] Department of Plant Protection, College of Agriculture, Bu-Ali Sina University, Hamedan, I.R. of Iran
[2] Iranian Research Institute of Plant Protection, Agricultural Research, Extension and Education Organization (AREEO), P.O. Box 1454, Tehran 19395, Iran

Summary. Between April and August 2013, two new fungal pathogens were isolated from strawberry foliage in strawberry production regions of Iran. Based on morphology and translation elongation factor 1-alpha (TEF) gene sequence analysis, the pathogens were identified as *Cladosporium macrocarpum* and *C. limoniforme*. Pathogenicity tests were performed on strawberry (*cv.* Parous) fruits and leaves and the original *C. macrocarpum* and *C. limoniforme* were re-isolated complying with Koch's postulates. This is the first report of *C. macrocarpum* and *C. limoniforme* as causal agents of a strawberry disease in Iran.

Key words: *Cladosporium macrocarpum, C. limoniforme, Fragaria ananassa*, taxonomy, *tef1*.

Strawberry (*Fragaria ananassa* Duch.) is an important small fruit crop grown worldwide, and its production is increasing steadily. Strawberry has been widely cultivated in the west and north of Iran for a long time. Fruit rot disease caused by fungi is one of the major problems to strawberry production and reducing their quantity and quality; causing economic losses in the fields at harvest time, during marketing and transportation (Embaby, 2007; Ayoubi and Soleimani, 2013). *Alternaria* spp., *Botrytis cinerea, Colletotrichum* spp., *Rhizoctonia solani, Phytophthora cactorum, Fusarium* spp., *Sclerotinia sclerotiorum*, and *Pestalotia longisetula* are the major fungal species causing strawberry fruit rots in many parts of the world (Embaby, 2007; Ayoubi and Soleimani, 2013; 2016a; 2016b). In Iran, *Botrytis cinerea* and *Colletotrichum acutatum* (Ayoubi and Soleimani, 2013) are the major causes of strawberry diseases, reducing fruit quantity and quality. Also, some *Fusarium* species (Ayoubi and Soleimani, 2016b) and *Neopestalotiopsis* spp. (Ayoubi and

Soleimani, 2016a) were recorded as fruit rot disease on strawberry, in recent years.

Moreover, recent observation indicated some other specific symptoms on strawberry leaves and fruits. In the field, symptoms are generally found on three major parts of strawberry, flowers, fruits and leaves. Under humid conditions, on the strawberries gray fungal colonies appeared and then the entire tissue underwent necrosis and turned into black rot. The pathogen caused green-gray sporulation on dead tissues and malformed or misshapen fruits. Black scab and dark brown sooty patches were observed on leaves in the greenhouse. The aim of the present study was to identify the causal agent that might be responsible for strawberry fruit rot, scab and flower blight.

Infected strawberry leaves, fruits and flowers (cv. Parous, Kurdistan and others) with typical symptoms (Figures 1a, 1b) were collected from commercial strawberry fields in Kurdistan province, Iran, from April to August 2013. Ten leaf, fruit and flower samples were collected from eight different locations; three infected fields around Sanandaj, three from Sarvabad and the other two from commercial strawberry fields in Kamyaran area.

Corresponding author: M.J. Soleimani
E-mail: j_soleimaniuk@yahoo.co.uk

Figure 1. Symptoms of disease on leaves, fruits and flowers by *Cladosporium macrocarpum* and *C. limoniforme* in the field. (a) Black sooty mold symptoms on leaves. (b) Flower and fruit blight. (c–f) Fruit rot stages induced by *C. macrocarpum* in pathogenicity test starting from achenes. *(g–h)* Symptoms on strawberry inoculated with a conidial suspension of *C. limoniforme*, g. on leaf, h. on fruits.

Conidia and conidiophores typical of *Cladosporium* were frequently observed on the diseased tissues under natural field conditions and also on the surfaces of disinfected leaf tissues kept in a humid chamber for 48 h at 25 ± 2°C with a 12-h photoperiod.

Isolates were consistently obtained from diseased tissues on Potato Dextrose Agar (PDA) at 24 ± 2°C. *Cladosporium* isolates were divided into two groups
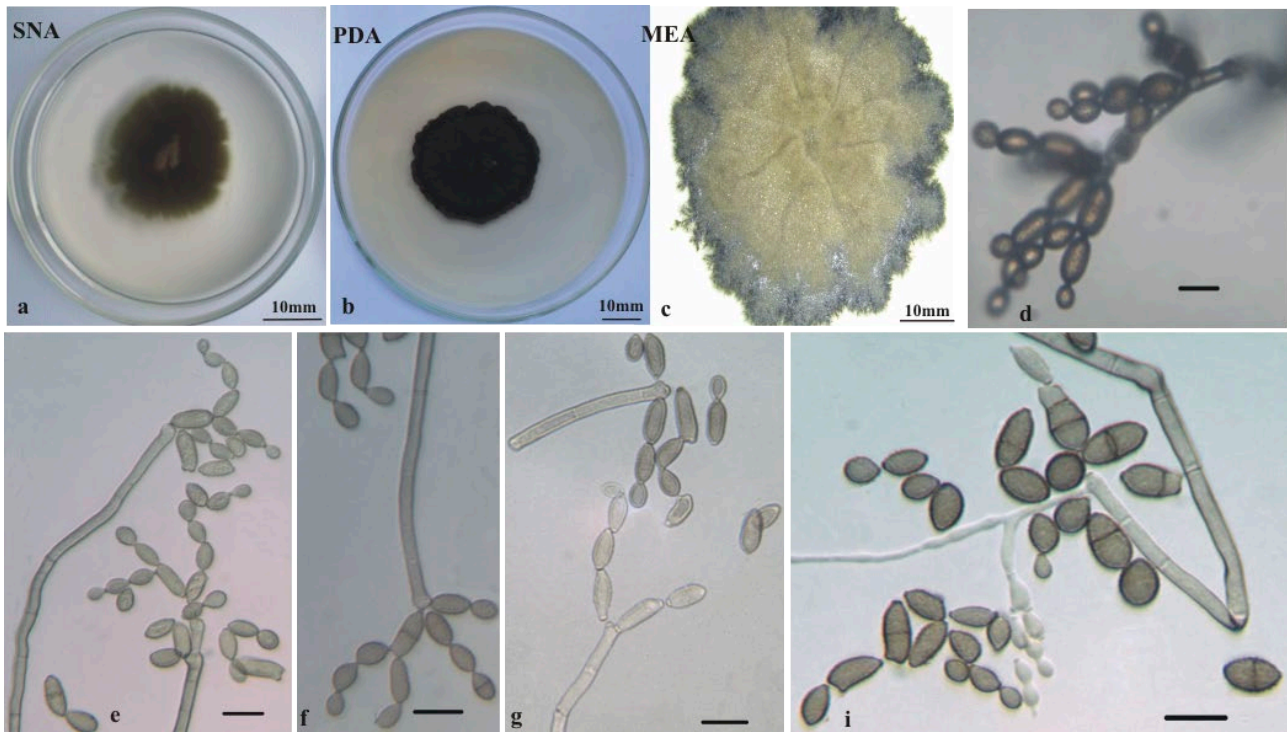
Figure 2. *Cladosporium macrocarpum*: (a) Colony on SNA, (b) colony on PDA, (c) colony on MEA. (d) Conidial chain. (e, f) Macronematous conidiophores and conidia. (g, h) Macro- and micronematous conidiophores and conidia. Scale bar = 10 μm.

based on colony morphology and colors on PDA, SNA (Synthetic Nutrient-poor Agar) and 2% MEA (Malt Extract Agar). Morphological observations were carried out on SNA incubated under continuous near-ultraviolet light at 25°C as described by Bensch *et al.* (2012). Conidia and conidiophores were mounted in distilled water and observed with an Olympus digital camera installed on a BX50 Olympus light microscope. The lengths and widths were measured using Digimizer. v. 4.1.1.0 software. Whenever possible, more than 30 measurements were made. For morphological structures such as conidia and conidiophores; mean, minimum, maximum and standard deviation were calculated. Representative isolates of the species obtained in this study were deposited in the culture collection of the Westerdijk Fungal Diversity Center (CBS 139754 and CBS 139755).

Nineteen monoconidial *Cladosporium* cultures were obtained in this study. Based on morpho-cultural characteristics, these isolates were assigned to two morphological groups (A, B). Eleven isolates belonged to group A, with CBS 139754 (Clad) as representative isolate, and eight isolates belonged to group B, with CBS 139755 (N 512) as representative. Isolates of group A formed on PDA dark dull green to olivaceous-gray colonies with dark olivaceous reverse; colonies were velvety with regular margin, reaching 20–35 mm diam after 10 d at 25°C. Colonies on MEA were olivaceous-gray, sometimes pale olivaceous-gray to white, reaching 40–50 mm diam. in 10 d at 25°C. On SNA these isolates formed olivaceous-gray to dark smoke-gray colonies with olivaceous-black reverse, reaching 15–25 mm diam. after 10 d at 25°C. Conidiophores were micronematous and macronematous, solitary. Macronematous conidiophores were erect, oblong-cylindrical, nodulose to nodose, sometimes distinctly geniculate, unbranched or sometimes branched, 11–285 × 3.5–6 μm, with swellings 5.5–10 μm wide, pale to medium brown or olivaceous-brown. Micronematous conidiophores were almost indistinguishable from hyphae, straight, 10–55 × 2–3 μm, sub-hyaline and smooth. Conidia were catenate, in branched chains; terminal conidia small, subglobose, obovoid, oval to limoniform, 4–8 × 4–5.7 μm [av. 6.5 × 4.8 μm] and aseptate; intercalary conidia broadly ovoid-ellipsoid, 9.2–15.5 × 5–6.5 μm [av. 11.5 × 5.7 μm] and 0–1-septate;
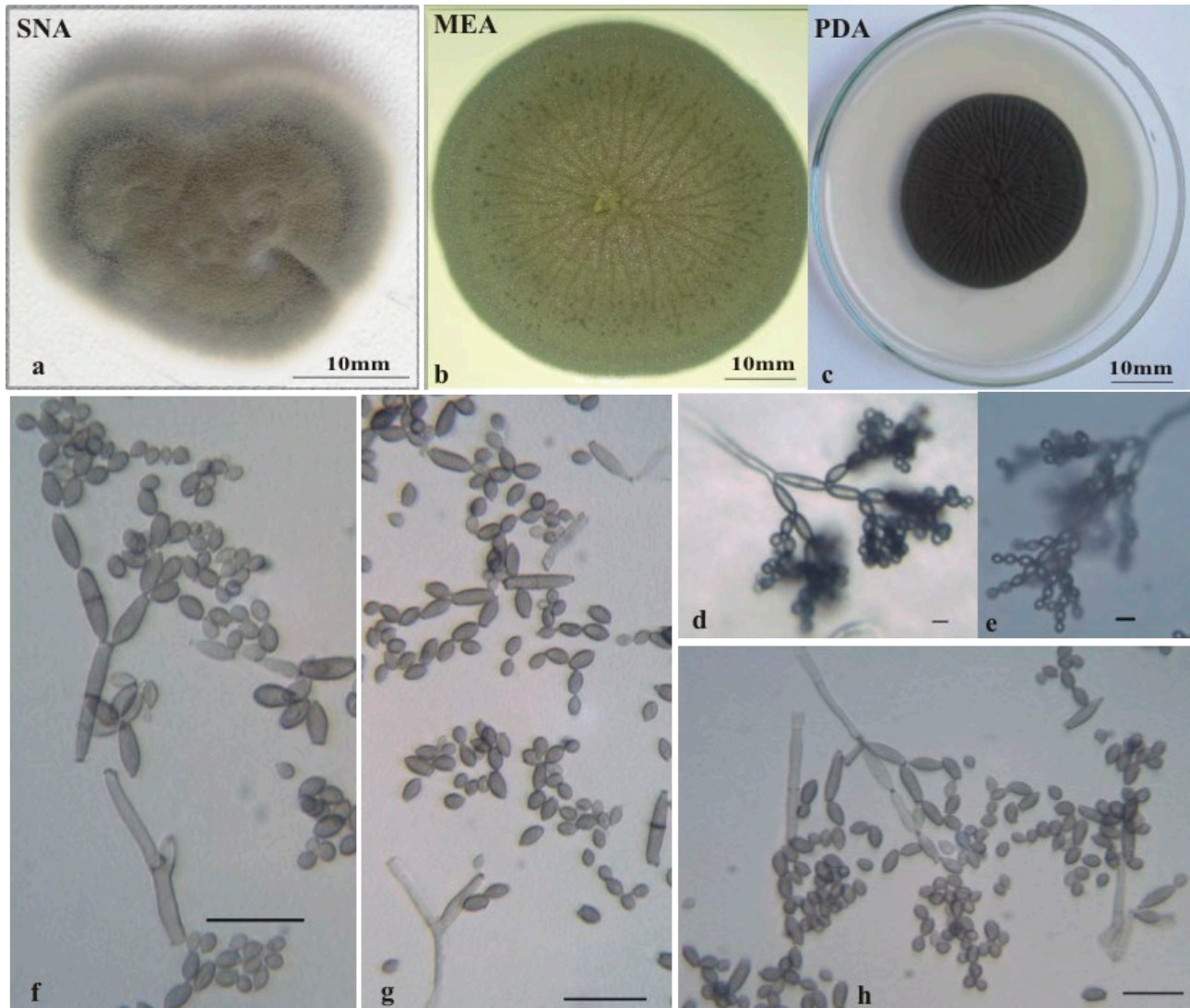
Figure 3. *Cladosporium limoniforme*: (a) Colony on SNA. (b) colony on PDA. (c) Colony on MEA. (d, e) Conidial chains. (f, g, h) Micronematous conidiophores forming large numbers of conidia. Scale bar = 10 µm.

ramoconidia were 20–24 × 2.3–2.5 µm, 0(–1)-septate; secondary ramoconidia broadly ellipsoid to subcylindrical, 13–22(–30) × 5–8.5 µm [av. 19 × 6.8 µm] and 0–2(–3)-septate (Figure 2a–2h).

Isolates of group B formed smoke-gray to dark gray-olivaceous, velvety to granular colonies with regular margins on PDA, attaining 20–40 mm diam in 10 d. Colonies on MEA were gray-olivaceous, greenish olivaceous to smoke-gray, reaching 40–55 mm diam in 10 d. Colonies on SNA were gray-olivaceous to olivaceous and velvety, reaching 25–

35 mm diam. Conidiophores were micronematous to semi-macronematous, sometimes macronematous, short, unbranched, sometimes hardly distinguishable from hyphae, usually neither geniculate nor nodulose, rarely once geniculate, measuring 7–85 × 1–3.5 µm. Conidia were catenate, pale olivaceous-brown or pale brown; small terminal conidia were obovoid to subglobose, apex rounded, attenuated towards the base, 1.3–4 × 1.1–2.3 µm [av. 2.5 × 1.8 µm], aseptate; intercalary conidia were limoniform, ovoid to ellipsoid, 3–9(–12) × 1.2–3.5 µm [av. 2 × 5
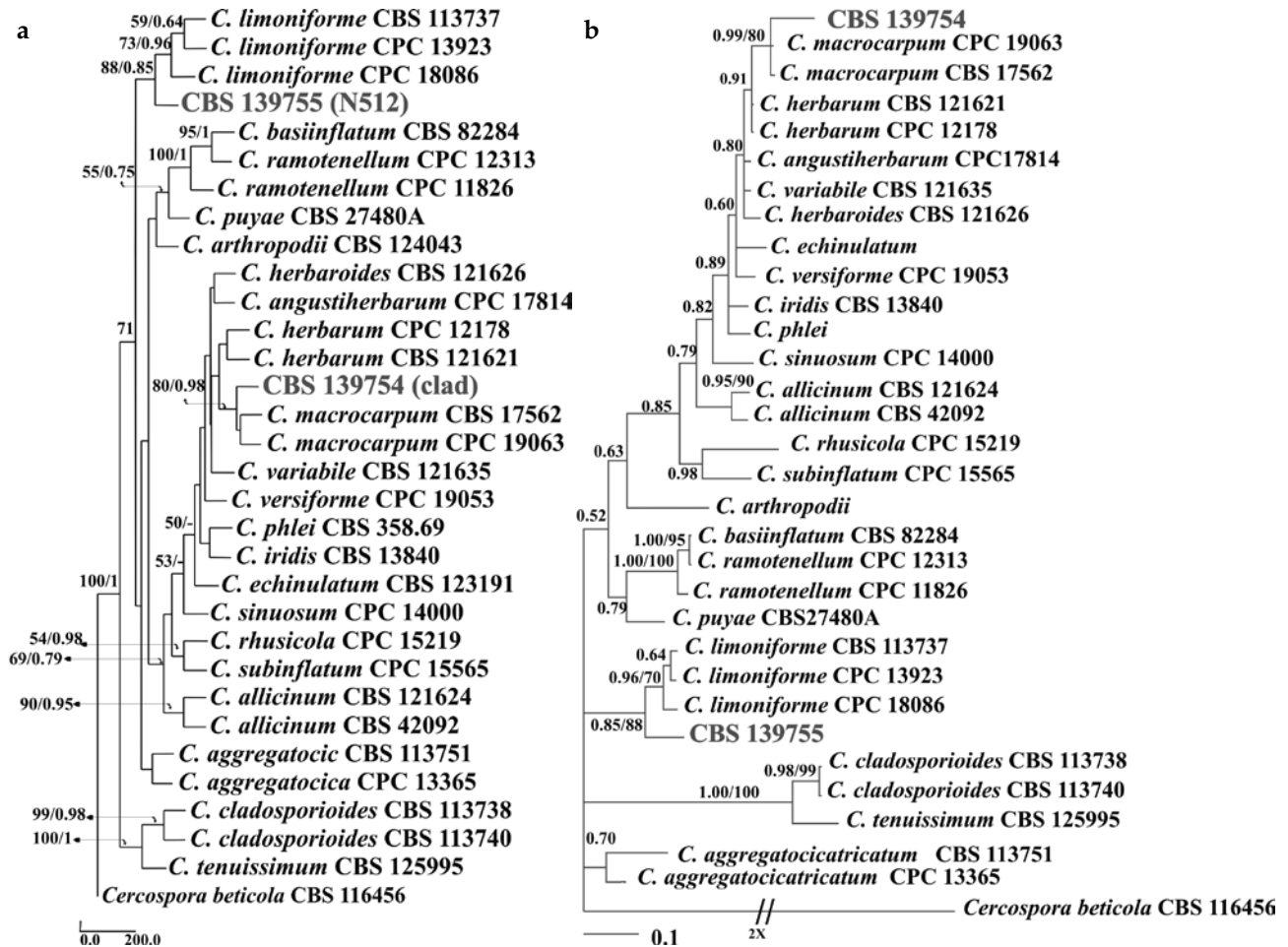
Figure 4. Phylogram generated from Maximum Parsimony (a) and Bayesian analysis (b) based on Tef1 sequences of selected *Cladosporium* species from NCBI and our new isolates. Maximum Parsimony Bootstrap (MPB) support values greater than 50% and Bayesian Posterior Probabilities (PP) greater than 0.75 are indicated above the nodes of each tree. The isolates obtained in this study are shown in bold and red. The scale bar represents the expected number of changes per site. The tree was rooted to *C. tenuissimum* CBS 125995, *C. cladosporioides* CBS 113738 and CBS 113740.

µm], aseptate; ramoconidia were 13–20 × 2–2.3 µm, 0(–1)-septate; scondary ramoconidia were ellipsoid to subcylindrical, 5–13 × 1.6–2.5 µm [av. 8 × 2 µm], 0–1-septate (Figures 3a–3h).

The cultural and morphological characteristics of CBS 139754 were consistent with the published descriptions of *Cladosporium macrocarpum* Preuss (Bensch *et al.*, 2012), whereas, CBS 139755 matched *C. limoniforme* Bensch, Crous & U. Braun (Bensch *et al.*, 2015).

Cladosporium macrocarpum and *C. limoniforme* belong to the *C. herbarum* complex, in which, according to Bensch *et al.* (2015), *tef1* gene sequences are sufficient to adequately distinguish species. For

molecular identification, mycelium was harvested from Potato Dextrose Broth (PDB) cultures and DNA was extracted using a CTAB procedure before being subjected to PCR. The partial gene sequences of the translation elongation factor 1-α gene (*EF-1α*) were amplified using primers EF1-728F and EF1-986R (Carbone & Kohn 1999) and a program described by Bensch *et al.* (2012). A commercial sequencing facility (Macrogen, Seoul, Korea) provided the sequences. Sequences were analysed with the basic sequence alignment BLAST program run against the NCBI database (National Center for Biotechnology Information website, http://www.ncbi. nlm.nih.gov).

Table 1. List of isolates used to infer the phylogenetic tree. The isolates used in this study are shown in bold.

GenBank *tef1* No.	Country	Host	Strain No.	Species
KT600551	Germany	*Asteriscus sericeus*	CPC 13365	*C. aggregatocicatricatum*
EF679425	Belgium	*Hordeum vulgare*	CBS 121624	*C. allicinum*
KT600466	Germany	*Acer campestre*	CBS 420.92	
KT600475	USA: Utah	*Pinus ponderosa*	CPC 17814	*C. angustiherbarum*
JN906985	New Zealand	*Arthropodium cirratum*	CBS 124043;	*C. arthropodii*
HM148241	Germany	*Hordeum vulgare*	CBS 822.84	*C. basiinflatum*
HM148245	USA	Grape bud	CBS 113738	*C. cladosporioides*
HM148247	USA	Grape berry	CBS 113740	
JN906987	New Zealand	*Dianthus barbatus*	CBS 123191	*C. echinulatum*
EF679432	Israel	Hypersaline water	CBS 121626	*C. herbaroides*
EF679440	The Netherlands	*Hordeum vulgare*	CBS 121621	*C. herbarum*
EF679441	The Netherlands	*Hordeum vulgare*	CPC 12178	
EF679447	The Netherlands	*Iris* sp.	CBS 138.40	*C. iridis*
KT600493	USA	Grape berry	CBS 113737	*C. limoniforme*
KT600498	Cyprus	*Eucalyptus* sp.	CPC 13923	
KT600499	—	Tomato	CPC 18086	
KT600497	Israel	Hypersaline water	CPC 12050	
KT600494	Egypt	*Musa acuminata*	CBS 140484 = CPC 12039 (ex-type)	
KT600495	Israel	Hypersaline water	CPC 12048	
KT600496	Israel	Hypersaline water	CPC 12049	
KU738715	**Iran**	***Fragaria × ananassa***	**CBS 139755; N512**	
KT600502	The Netherlands	*Hordeum vulgare*	CBS 175.62	*C. macrocarpum*
KT600503	Iran	*Hordeum* sp.	CPC 19063	
KT600501	Morocco	*Diospyros kaki*	CBS 108.85	
EF679453	USA	*Spinacia oleracea*	CBS 121623 (ex-neotype)	
KU738714	**Iran**	***Fragaria × ananassa***	**CBS 139754; Clad**	
KT600516	Colombia	*Puya goudotiana*	CBS 274.80A	*C. puyae*
JN906991	Germany	*Phleum pratense*	CBS 358.69	*C. phlei*
KT600539	South Africa	*Rhus* sp.	CBS 140492	*C. rhusicola*
KT600528	Germany	*Rosa* sp.	CPC 12313	*C. ramotenellum*
KT600525	USA	*Phyllactinia guttata*	CPC 11826	
KT600542	South Africa	Wheat	CPC 14000	*C. sinuosum*
KT600546	Ukraine	*Iris* sp.	CPC 15565	*C. subinflatum*
HM148442	USA, Louisiana	*Lagerstroemia* sp.	CBS 125995	*C. tenuissimum*
EF679480.1	USA	*Spinacia oleracea*	CBS 121635	*C. variabile*
KT600515	Iran	*Hordeum* sp.	CBS 140491	*C. versiforme*

Sequences of two representative isolates recovered in this study as well as related sequences retrieved from GenBank were aligned using CLUSTALX2 (Thompson *et al.*, 1997). The aligned dataset was analysed with Bayesian Inference (BI) and Maximum Parsimony (MP). Suitable models for the Bayesian analysis were first selected using models of nucleotide substitution for each gene, using MrModeltest version 3.6 (Nylander, 2004). The Bayesian analyses [MrBayes v. 3.2.1; 22] were run from random trees for 800,000 generations and sampled every 100 generations. The MP analysis was performed with PAUP* (Phylogenetic Analysis Using Parsimony) v. 4.0b10 (Swofford, 2003). Trees were inferred by using the heuristic search option with TBR branch swapping and 1,000 random sequence additions. Tree length [TL], consistency index [CI], retention index [RI], rescaled consistency index [RC], and homoplasy index [HI] were calculated. The robustness of the equally most parsimonious trees was evaluated by 1,000 bootstrap replications, resulting from a maximum parsimony analysis, each with 10 replicates of random stepwise addition of taxa. The resulting trees were printed with Treeview (Page, 1996). *Cladosporium tenuissimum* CBS 125995, *C. cladosporioides* CBS 113738 and CBS 113740 were used as outgroups. The sequences of the amplified products are deposited in the GenBank database (Table 1).

Multiple alignment was carried out with Clustal X using default parameters (Thompson *et al.,* 1997). Dirichlet base frequencies and the GTR+I+G model were recommended by the MrModeltest (Nylander, 2004) to be used in the Bayesian analysis. The 50% consensus trees and posterior probabilities were calculated from the trees left after discarding the first 25% of generations for burn-in.

The parsimony analysis indicated that 169 characters were constant, 31 variable characters parsimony-uninformative and 125 characters parsimony-informative. After a heuristic search using PAUP*, 7 most parsimonious trees were obtained (tree length = 414 steps, CI = 0.518, RI = 0.815, RC = 0.486, HI = 0.403). CBS 139754 was placed in the same clade with CBS 121623, the ex-neotype isolate of *C. macrocarpum* and other isolates of this species (downloaded from NCBI) with Posterior Probability (PP) 1 and 99% Maximum Parsimony Bootstrap (MPB); CBS 139755 clustered with CPC 12039 = CBS 140484, the ex-type of *C. limoniforme* and other isolates of this species (PP = 1 and MPB = 100%) (Figure 4). The isolates used to draw the phylogenetic tree are listed in Table 1.

Based on the symptoms, fungal morphology, and *EF-1α* sequences, our isolates were identified as *C. macrocarpum* and *C. limoniforme.*

Several species of the genus *Cladosporium* have been reported from strawberry. Occurrence of blossom blight in strawberry during harvesting was first reported to be caused by *Cladosporium cladosporioides* in California, USA (Gubler *et al.*, 1999). In Korea, the occurrence of *Cladosporium* spp. in strawberry was reported as scabs on the leaf, calyx, and runner caused mostly by *C. herbarum* (Kwon *et al.*, 2001). The occurrence of *C. cladosporioides* and *C. tenuissimum* in Korea was reported as strawberry blossom blight (Nam *et al.*, 2015). But, *C. macrocarpum* and *C. limoniforme* have not yet been reported from strawberry. *C. macro-carpum*, a second component within the *C. herbarum* species complex, has been previously isolated from decaying plant materials, human substrates, hypersaline water (Schubert *et al.*, 2007), and also from *Prunus avium* (Dugan and Roberts, 1994) and *Sorghum bicolor* (Kortei *et al.*, 2015). According to Bensch *et al.* (2015), *C. limoniforme* belongs to the *C. herbarum* species complex, species of which were isolated from plant material and hypersaline water in Africa (Egypt), Asia (Israel), Europe (Cyprus) and North America (USA).

For pathogenicity tests, spore suspensions (1000 conidia mL^{-1}) of each isolate were sprayed onto 10 healthy, detached strawberry fruits and leaves. An equal number of healthy strawberry fruits and leaves were simultaneously sprayed with sterilized distilled water as control. The tissues were then incubated in a growth chamber at 25°C and >70% relative humidity. Daily observations were made on the development of disease symptoms. After 10 days, spores from diseased tissues were aseptically transferred onto PDA plates. The resultant cultures were checked for colony and spore morphology to comply with Koch's postulates.

Symptoms of the disease were similar to those observed in the field after inoculating isolates of our species (CBS 139754 or CBS 139755) (Figures 1c–1h). Both species caused severe damage on strawberry fruits and leaves. Initial symptoms of fruit lesions and scab appeared 6–8 days after inoculation, followed by leaf spots after 10–12 days. The infected tissues were usually surrounded by dark green or dark gray soot on the lesions. Symptoms of *C. macrocarpum* on fruits started from achenes on which a gray fungus was visible under the binocular. Eventually the entire fruit became

malformed and turned into black rot (Figure 1c–1f). Control tissues were asymptomatic. Representative isolates were successfully re-isolated from symptomatic tissue in line with Koch's postulates. To our knowledge, this is the first report of Cladosporium scab and blight on leaves and fruits of strawberry in Iran.

Acknowledgment

Literature cited

Ayoubi N. and M.J. Soleimani, 2013. Occurrence of strawberry anthracnose disease caused by *Colletotrichum acutatum* in Kurdistan province. 1st Iranian Mycological Congress, 3-5 September, University of Guilan, Rasht, Iran, pp. 97.

Ayoubi N. and M.J. Soleimani, 2016a. Strawberry fruit rot caused by *Neopestalotiopsis iranensis* sp. nov., and *N. mesopotamica. Current Microbiology* 72, 329–336.

Ayoubi N. and M.J. Soleimani, 2016b. Morphological and molecular identification of pathogenic *Fusarium* spp. on strawberry in Iran. *Sydowia* 68, 163–171.

Bensch K., U. Braun, J.Z. Groenewald, and P.W. Crous, 2012. The genus *Cladosporium. Studies in Mycology* 72, 1–401.

Bensch K., J.Z. Groenewald, U. Braun, J. Dijksterhuis, M. de Jesús Yáñez-Morales and P.W. Crous, (2015). Common but different: The expanding realm of *Cladosporium. Studies in Mycology* 82, 23–74.

Carbone I. and L.M. Kohn, 1999. A method for designing primer sets for speciation studies in filamentous *ascomycetes. Mycologia* 91, 553–556.

Dugan F.M., R.G. Roberts, 1994. Morphological and reproductive aspects of *Cladosporium macrocarpum* and *C. herbarum* from bing cherry fruits. *Mycotaxon* 52, 513–522.

Embaby E., 2007. Pestalotia fruit rot on strawberry plants in Egypt. *Egyptian Journal of Phytopathology* 35, 99–110.

Gubler W.D., A.J. Feliciano, A.C. Bordas, E.C. Civerolo, J.A. Melvin and N.C. Welch, 1999. First report of blossom blight of strawberry caused by *Xanthomonas fragariae* and *Cladosporium cladosporioides* in California. *Plant Disease* 83, 400.

Kortei N.K., G.T. Odamtten, V. Appiah, M. Obodai, A. Adu-Gyamfi and M. Wiafe-Kwagyan, 2015. Comparative occurrence of resident fungi on gamma irradiated and steam sterilized sorghum grains (*Sorghum bicolor* L.) for spawn production in Ghana. *British Biotechnology Journal* 7(1), 21–32.

Kwon J.H., S.W. Kang, J.S. Kim and C.S. Park, 2001. Occurrence of strawberry scab caused by *Cladosporium herbarum* in Korea. *Mycobiology* 29, 110–112.

Nam M.H., M.S. Park, H.S. Kim, T.I. Kim and H.G. Kim, 2015. *Cladosporium cladosporioides* and *C. tenuissimum* cause blossom blight in strawberry in Korea. *Mycobiology* 43(3), 354–359.

Nylander J.A.A., 2004. MrModeltest v2. Program distributed by the author. Evolutionary Biology Centre, Uppsala University.

Page R.D.M., 1996. TREEVIEW: an application to display phylogenetic trees on personal computers. *Computer Applications in the Biosciences* 12, 357–358.

Schubert K., J.Z. Groenewald, U. Braun, J. Dijksterhuis, M.S. Starink, C.F. Hill, P. Zalar, G.S. de Hoog and P.W. Crous, 2007. Biodiversity in the *Cladosporium herbarum* complex (*Davidiellaceae, Capnodiales*), with standardisation of methods for *Cladosporium* taxonomy and diagnostics. *Studies in Mycology* 58, 105–156.

Swofford D.L., 2003. PAUP*. Phylogenetic analysis using parsimony (* and other methods). Version 4.

Thompson J.D., T.J. Gibson, F. Plewniak, F. Jeanmougin and D.G. Higgins, (1997). The CLUSTAL_X windows interface: flexible strategies for multiple sequence alignment aided by quality analysis tools. *Nucleic Acids Research* 25, 4876–4882.